Novel Fe-based complex oxide catalysts for hydroxylation of phenol

Chunrong Xiong [a], Qingling Chen [a,*], Weiran Lu [a], Huanxin Gao [a], Wenkui Lu [a] and Zi Gao [b,*]

[a] *Shanghai Research Institute of Petrochemical Technology, Shanghai 201208, PR China*
[b] *Department of Chemistry, Fudan University, Shanghai 200433, PR China*

Received 2 May 2000; accepted 15 August 2000

Novel catalysts for the hydroxylation of phenol, Fe–Si–O, Fe–Mg–O and Fe–Mg–Si–O complex oxides, have been synthesized by a coprecipitation method. X-ray diffraction studies show that $MgFe_2O_4$ crystallites with spinel structure are formed in Fe–Mg–Si–O and Fe–Mg–O complex oxides and the crystallite size of the metal oxide or complex oxide is reduced after addition of Si. In the hydroxylation of phenol with hydrogen peroxide, Fe-based complex oxides exhibit high activities after a short induction period. The phenol conversion is improved when silicon is introduced into the Fe-based complex oxides, and formation of $MgFe_2O_4$ crystals with spinel structure in the catalysts increases the diphenol selectivity. The addition of a little acetic acid to the reaction liquid can shorten the induction period effectively. Under the same reaction conditions, phenol conversion and diphenol selectivity over the Fe–Mg–Si–O catalyst are close to those over TS-1, and furthermore, the reaction time is more than ten times shorter as compared to TS-1. The reaction mechanism of the hydroxylation of phenol on the catalysts has been studied, and a free-radical mechanism initiated by the formation of phenoxy free radicals is suggested.

Keywords: Fe-based complex oxide, spinel, hydroxylation of phenol, diphenol

1. Introduction

Diphenol is an important intermediate chemical in agrochemical and fine chemical industries, and much attention is still being paid to the production of diphenol. $HClO_4$–H_3PO_4 [1] and Fe(III)/Co(II) [2] catalysts are used conventionally, but obvious shortcomings of these homogeneous catalysts prevent their wide use in diphenol production. To date, many researchers have been interested in the development of heterogeneous catalysts for hydroxylation of phenol in the liquid phase with aqueous H_2O_2. The catalysts used are mostly transition-metal-containing zeolites, such as TS-1 [3,4], TS-2 [5,6], Ti-β [7], Ti-MCM-41 [8], V-ZSM-11 [9] and Cu-ZSM-5 [10]. However, as far as these microporous molecular sieves are concerned, despite the attractive catalytic activities shown by some of them, these materials are often expensive and relatively difficult to synthesize. Besides, their slower reaction rate also limits their wide application in industrial production. Attempts have been made to replace these zeolite-based catalysts with heteropolyacids such as molybdovanadophosphoric acid [11] and molybdotungstophosphoric acid [12], but the decomposition of H_2O_2 over these catalysts is very obvious, and acetonitrile is the only applicable solvent. It was also reported that simple metal oxides or supported metal oxides could catalyse phenol hydroxylation, e.g., Fe_2O_3 [13], Co_3O_4 [14], CuO/SiO_2 [15], Fe_2O_3/Al_2O_3 [16], MoO_3 [17], V_2O_5 and TiO_2 colloidal particles [18], but all these oxides had poor catalytic activity and low diphenol selectivity. Complex oxides containing transition metals, such as $La_{1.9}Sr_{0.1}CuO_{4\pm\lambda}$ [19] and V–Zr–O [20,21], were used for hydroxylation of phenol as well, however, both their diphenol yield and reaction rate were low. Iron oxide nanoparticles [22], prepared inside the pores of macroporous resins by *in situ* forced hydrolysis of Fe^{3+} ions chemisorbed at the pore walls, show hydroxylation activity, but the active component of such catalyst is lost easily, and the phenol conversion of the catalyst is not high enough.

In the present paper, we will report synthesis, characterization and catalytic reaction data for phenol hydroxylation of three kinds of Fe-based complex oxide. The catalysts are cheap and their preparation method is simple. These new catalysts show not only a good catalytic performance, but also quite a speedy reaction rate in the hydroxylation of phenol with aqueous hydrogen peroxide solution due to an involvement of a possible heterogeneous–homogeneous free-radical reaction mechanism. The catalysts are also active in the hydroxylation of benzene and the oxidation products are phenol, catechol and hydroquinone, which will be reported later on.

2. Experimental

2.1. Preparation of catalyst

Four different Fe-based complex oxide samples were prepared by coprecipitation with ammonia. For preparing Fe–Mg–Si–O (atomic ratio $Fe:Mg:Si = 2.2:1:1$), desired amounts of $Fe(NO_3)_3{\cdot}9H_2O$, $Mg(NO_3)_2{\cdot}6H_2O$ and

* To whom correspondence should be addressed.

silica gel were placed in a round-bottom flask equipped with a thermometer and magnetic stir bar, and distilled water was added into the flask. After stirring for 30 min, the mixed liquid was heated to 70 °C, and aqueous ammonia solution was dropped in slowly. The precipitate was filtrated, washed with distilled water, dried at 120 °C for 8 h, triturated into powder and calcined at 800 °C for 4 h. Fe–Mg–O (atomic ratio Fe : Mg = 2.2 : 1), Fe–Si–O (atomic ratio Fe : Si = 1.83 : 1) and α-Fe_2O_3 samples were prepared similarly using corresponding raw materials.

2.2. Hydroxylation of phenol

Hydroxylation of phenol was conducted in a 250 ml batch reactor with stirring. 5.6 g phenol, 50 ml distilled water and 0.28 g catalyst were placed in the reactor, and the reaction was carried out under reflux condition (ca. 70 °C). At the beginning of the reaction 2 ml of 30 wt% H_2O_2 was added into the reaction mixture and the reaction was monitored by taking a small amount of sample (0.2 ml) at different times. The reaction products were analyzed by high-pressure liquid chromatography (HP 1090). A column (ODS Hypersil 5 μm, 100 × 4.6 mm) with methanol/water (30/70, 0.4 ml/min) as an eluent was used. Detection was done by a UV detector at 280 nm.

2.3. Characterization

X-ray powder diffraction (XRD) was performed on a D/max1400 X-ray diffractometer with Cu Kα radiation and a Ni filter. The spectra were recorded between 10° and 70° and a scanning rate of 15°/min was used. TPR studies were carried out using a Micromeritics TPD/TPR 2900 instrument. For TPR experiments, about 15 mg of catalyst was pretreated at 400 °C in Ar for 3 h, the temperature was lowered to room temperature, a gas mixture of 10% H_2 in Ar was passed over the catalyst, and then the temperature was raised at a rate of 10 °C /min up to 800 °C. BET surface areas of the catalysts were measured on a Micromeritics ASAP 2000 system under liquid-N_2 temperature using N_2 as the adsorbate.

3. Results

3.1. Catalyst properties

X-ray diffraction patterns of the samples are presented in figure 1. Five strong peaks at 30.2°, 35.4°, 43.1°, 56.9° and 62.5° and two weak peaks at 37.1° and 53.5° appear in the pattern of the Fe–Mg–O complex oxide, which can be assigned, respectively, to the (220), (317), (400), (511), (440), (212) and (422) diffraction peaks of $MgFe_2O_4$ crystallite with a spinel structure. The low background signal and the sharpness of the peaks indicate a high crystallinity of the spinel structure. There are also weak reflections in the pattern of Fe–Mg–O at 24.3°, 33.3°, 41.0°, 49.5°, 54.2° and 64.2°, suggesting a small amount of α-Fe_2O_3 phase is present in the sample as well. While magnesia belongs to the same symmetry group and has exactly half the lattice parameter of the spinels, a separate MgO phase is not observed in the patterns [23]. In the XRD pattern of Fe–Mg–Si–O the five strong peaks characteristic of the spinel structure are broadened and the two weak peaks disappeared, indicating that the spinel structure in the sample has a smaller crystallite size than that in the Fe–Mg–O sample. The weak, broadened peaks of α-Fe_2O_3 indicate the crystallite size of the α-Fe_2O_3 phase of corundum structure in the sample is reduced as well. The peak positions and the relative intensities of the peaks for the Fe–Mg–Si–O sample are the same as those for Fe–Mg–O, suggesting that the small $MgFe_2O_4$ and α-Fe_2O_3 crystallites in the sample are dispersed in a matrix of silica and the presence of the silica matrix prevents these crystallites from further growth. The XRD pattern of the Fe–Si–O sample is similar to that of α-Fe_2O_3, but the reflections are broadened, showing that small crystallites of α-Fe_2O_3 are formed and they are also dispersed in a silica matrix in the sample. The crystallite sizes of the $MgFe_2O_4$ spinel struc-

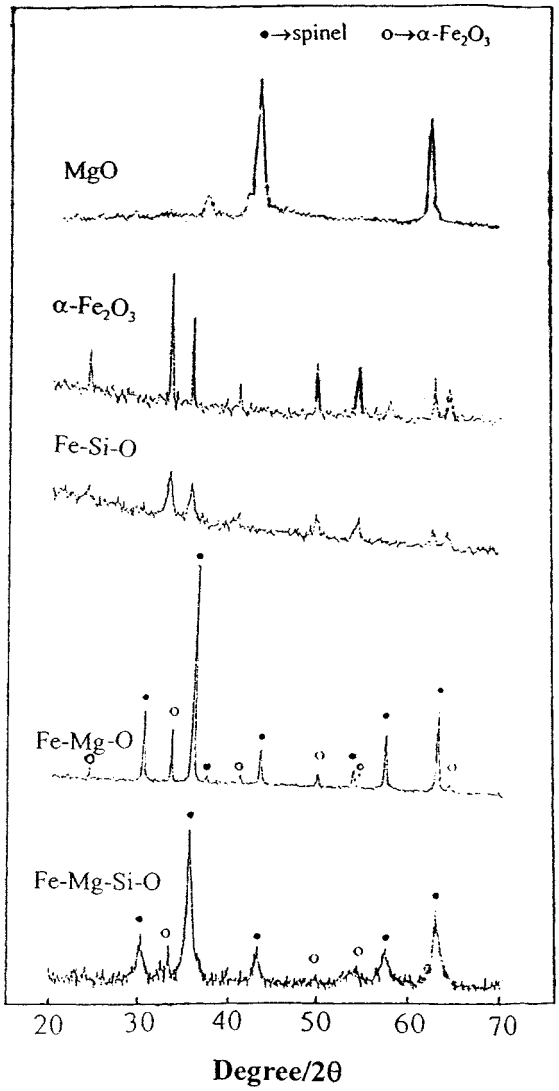

Figure 1. XRD patterns of the catalysts: (•) $MgFe_2O_4$ and (○) α-Fe_2O_3.

ture and the α-Fe_2O_3 corundum structure in the samples were calculated by Scherrer equation [24] and listed in table 1 together with the BET surface areas and pore volumes of the samples measured by the N_2 adsorption method.

The TPR profiles of the four different samples are shown in figure 2. For bulk α-Fe_2O_3, two peaks are observed at 434 and 570 °C which can be assigned to the reduction from Fe_2O_3 to Fe_3O_4 and Fe_3O_4 to Fe, respectively. The TPR profile of Fe–Si–O exhibits three peaks. The first two peaks occurring at 453 and 610 °C correspond to the two reduction steps of Fe_2O_3 as well, but both peaks shift to higher temperatures due to the smaller crystallite size of α-Fe_2O_3 in the sample. An additional peak is observed at 678 °C. It is probably associated to the reduction of Fe–O species strongly bound to the SiO_2 matrix [25]. Apparently, the two TPR profiles of Fe–Mg–O and Fe–Mg–Si–O are very similar due to the same crystal structure. They both have two small shoulder peaks and a large sharp peak, whose attribution needs to be investigated later on. One distinct difference observed is that the three peaks for Fe–Mg–Si–O appear at higher temperatures (445, 591 and 738 °C) than those (407, 502 and 655 °C) for Fe–Mg–O, suggesting that the $MgFe_2O_4$ in the Fe–Mg–Si–O sample also has smaller crystallite size. The TPR results further confirm that adding silica gel into the metal salt solutions before precipitation with ammonia is an effective way to prepare metal oxide catalysts with high surface area, in which nano-sized metal oxide or spinel crystallites are dispersed in a silica matrix.

Table 1
Properties of the catalysts.

Catalyst	Surface area (m^2/g)	Pore volume (ml/g)	Crystallite size (nm)
α-Fe_2O_3	2.66	0.0039	89
Fe–Si–O	137	0.117	32
Fe–Mg–O	24.7	0.128	63
Fe–Mg–Si–O	118	0.318	21

3.2. Catalyst activity

The catalytic activities in phenol hydroxylation over different catalysts are displayed in table 2. Pure MgO and SiO_2 have no activity in phenol hydroxylation, but α-Fe_2O_3 is catalytically active. It is interesting to note that the conversion of phenol for Fe–Si–O and Fe–Mg–Si–O catalysts is

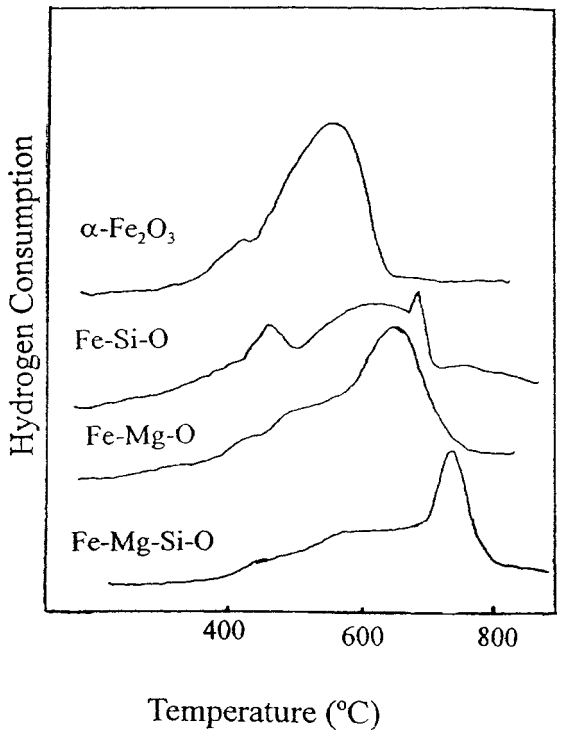

Figure 2. TPR profiles of the catalysts.

Table 2
Reaction characteristics of different catalysts.[a]

Catalyst	Phenol/ catalyst (g/g)	Phenol/ H_2O_2 (mol/mol)	Reaction time (h)	Phenol conv.[b] (%)	Selectivity to diphenol[c] (%)	Effective conv. H_2O_2[d] (%)	Selectivity to isomer[e] (%)		
							HQ	CAT	BQ
MgO	20	3	3	0	0	0	0	0	0
SiO_2	20	3	3	0	0	0	0	0	0
α-Fe_2O_3	20	3	3	13.4	77.1	31	37.0	56.7	6.3
Fe–Mg–O	20	3	1	21.7	97.5	63.6	40.9	58.9	0.2
Fe–Si–O	20	3	0.25	25.0	78.4	58.9	42.0	56.5	1.5
Fe–Mg–Si–O	20	3	0.5	24.5	94.3	69.2	45.9	53.6	0.5
Fe–Mg–Si–O	20	1	0.5	56.5	88.5	50.0	42.0	56.8	1.2
TS-1[f]	10	3	6	26.0	90.0	70.3	45.5	52.3	2.2
$La_{1.9}Sr_{0.1}CuO_{4\pm\lambda}$ [19]	20	1	2	40.8	–	–	40.6	56.9	2.5
V–Zr–O [20]	20	1	6	28.4	–	–	39.3	59.9	0.8
$Fe(AC)_3$	20	3	0.5	6.8	77.9	15.8	40.4	57.8	1.8
Fe_2O_3/resin [22]	20	3	2	22.1	90.5	60.3	38.5	57.0	4.8

[a] Reaction conditions: water as solvent, reaction temperature 65 °C, $c_{HAC} = 0.03$ mol/l.
[b] Phenol conversion (%) = (phenol consumed (mol)/phenol added (mol)) ×100%.
[c] Selectivity diphenol (%) = (diphenol (mol)/phenol consumed (mol)) ×100%.
[d] Effective conversion H_2O_2 (%) = (diphenol (mol)/H_2O_2 added (mol)) ×100%.
[e] HQ = hydroquinone, CAT = catechol, BQ = *para*-benzoquinone.
[f] TS-1 with Si/Ti = 20, acetone as solvent, reaction temperature 57 °C.

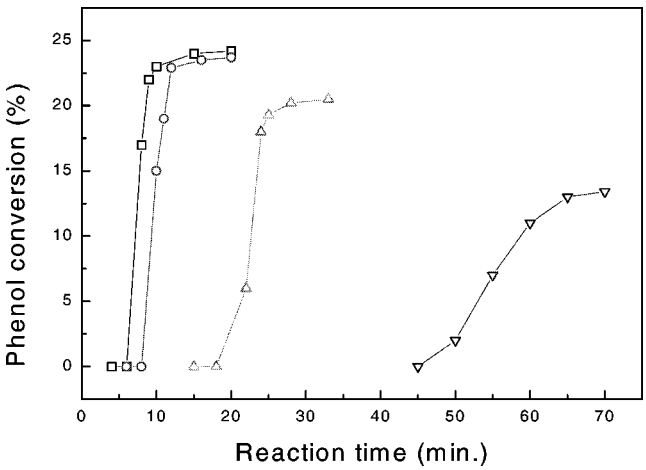

Figure 3. Plot of phenol conversion vs. reaction time for (□) Fe–Si–O, (○) Fe–Mg–Si–O, (△) Fe–Mg–O and (▽) α-Fe_2O_3.

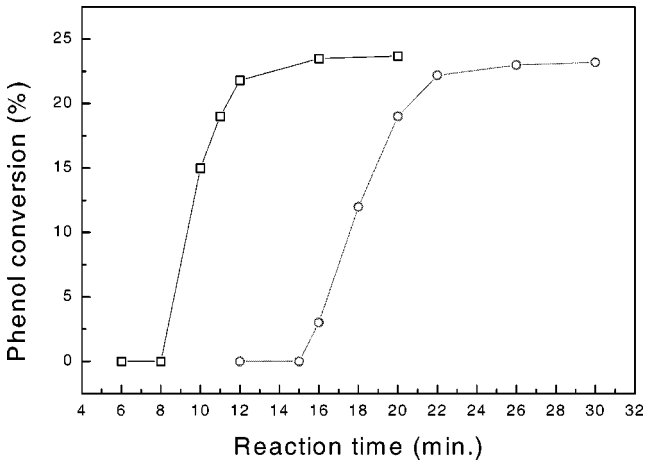

Figure 4. Influence of acetic acid on induction period over the Fe–Mg–Si–O catalyst: (□) adding 0.15 ml acetic acid and (○) without acetic acid.

higher than that for Fe–Mg–O and α-Fe_2O_3. Furthermore, the diphenol selectivity of the catalysts increases in the order of α-Fe_2O_3 < Fe–Si–O < Fe–Mg–Si–O < Fe–Mg–O. The reaction data of TS-1 and other catalysts reported in the literature are listed in table 2 for comparison. The phenol conversion of Fe–Si–O and Fe–Mg–Si–O is close to that of TS-1, and the diphenol selectivity of Fe–Mg–O and Fe–Mg–Si–O is higher than that of TS-1. Besides, the reaction time of Fe–Si–O, Fe–Mg–O and Fe–Mg–Si–O is much shorter than that of TS-1. Since the Fe–Mg–Si–O catalyst is much more cheaper and easier to prepare than TS-1, it is a new hopeful catalyst to replace TS-1 for diphenol production industry.

The increase of phenol conversion with time on stream over the catalysts is shown in figure 3. There is an induction period at the beginning of the reaction, and after the induction period phenol conversion increases exponentially. The induction period of the catalysts increases in the order of Fe–Si–O < Fe–Mg–Si–O < Fe–Mg–O < α-Fe_2O_3, suggesting that the length of the induction period is related not only to the nature of the active components but also to their crystallite size. Obviously, for the same kind of active species the smaller the crystallite size, the shorter the induction period.

It has also been noticed that adding a little amount of acetic acid into the reaction mixture can shorten the induction period of the reaction markedly, as shown in figure 4. Since no iron ions are detected in the solution, the acceleration of the reaction is not caused by the dissolution of the catalyst. Besides, a comparative reaction was run using $Fe(AC)_3$ as a catalyst, and the results are listed in table 2. The activity and selectivity of $Fe(AC)_3$ are much lower than those of the oxide catalysts. Thus, the real reason for the acceleration deserves further studies. When acetone, methanol, ethanol and isopropanol are used as the solvent for the reaction, the catalytic activity of the catalysts is reduced, which is probably due to the adsorption of these solvents on the active species of the catalysts.

4. Discussion

According to all of the above phenomena, a free-radical mechanism may be involved in phenol hydroxylation over this kind of catalysts. In the hydroxylation of phenol over complex oxide $La_{1.9}Sr_{0.1}CuO_{4\pm\lambda}$ [19] and oxidation of phenol over copper oxide [26], a heterogeneous–homogeneous free-radical reaction mechanism has been proposed. The heterogeneous–homogeneous reaction mechanism in liquid phase oxidation over solid catalysts was initially proposed by Mayer et al. [27]. In this type of reaction free radicals are formed on the surface of the solid catalysts and undergo propagation and termination in solution. In the case of phenol hydroxylation with hydrogen peroxide as oxidant, free radicals can be generated on the solid catalyst surface in two ways: (1) the catalyst accelerates the decomposition of hydrogen peroxide into radicals, or (2) the catalyst activates the phenol molecules directly, and facilitates the formation of phenoxy radicals. These two reaction mechanisms are described in schemes 1 and 2, respectively. It is assumed that the production of hydroquinone proceeds in the same manner as for catechol.

In scheme 1, the formation of $OH^{\cdot}$ radicals on the catalyst surface is the initiation step of the reaction, and the propagation of the reaction chain occurs in solution. Nevertheless, in scheme 2, phenoxy radicals are formed on the catalyst surface by hydrogen abstraction in the initiation reaction instead of hydroxyl radicals.

To explore which scheme is possible in phenol hydroxylation catalyzed by Fe-based catalysts, a series of experiments were designed and carried out in the lab. The reagents in the four reactors were different, as shown in figure 5. They were stirred and heated at 65 °C at the same initial time. After 10 min (longer than the induction period), 5 ml solution was transferred from reactor 1 into reactor 2 and from reactor 4 into reactor 3. At the same time, hydrogen peroxide and phenol were added into reactor 1 and reactor 4, respectively. It was observed that the reaction occurred immediately in reactor 1, whereas the reaction in reactor 4 started after an induction period. This suggested

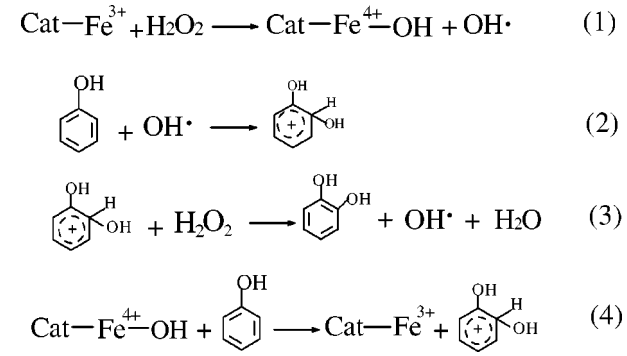

Scheme 1.

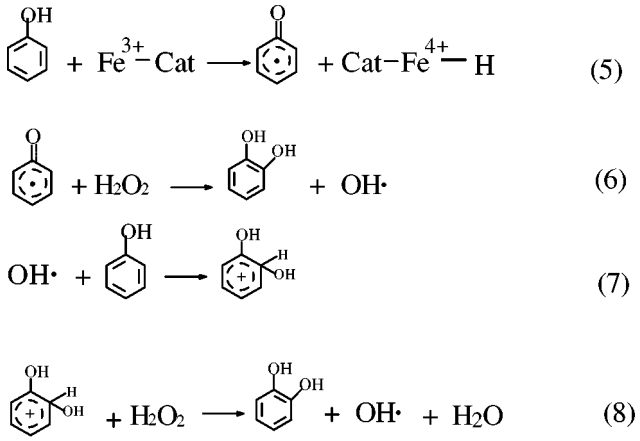

Scheme 2.

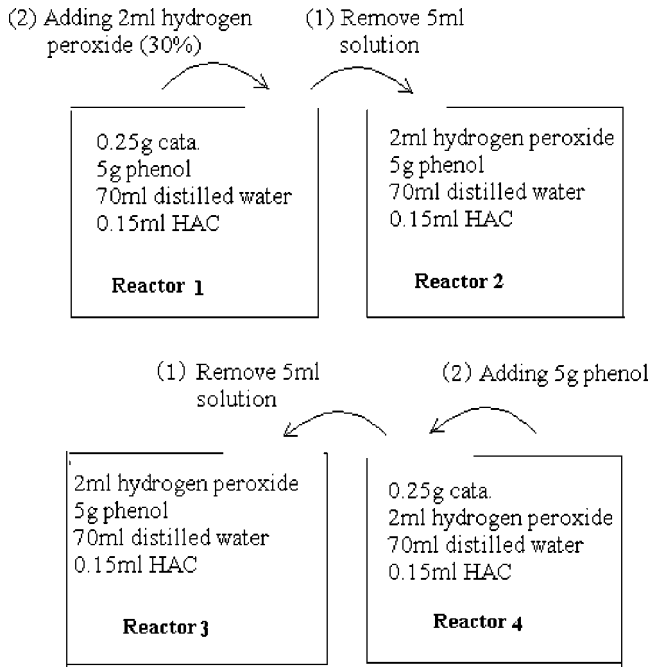

Figure 5. Designed experiments for phenol hydroxylation over Fe–Mg–Si–O catalyst.

that phenoxy radicals were formed on the Fe–Mg–Si–O catalyst in reactor 1 before addition of hydrogen peroxide, but the initiation reaction in scheme 1 did not occur in reactor 4 through the interaction of the catalyst and hydrogen peroxide. Since iron ions were not detected in the phenol solution of reactor 1, it could be confirmed that the hydroxylation reaction in the reactor was not catalyzed by iron ions originated from the dissolution of the catalyst, as described in [28,29]. Moreover, the solution was darkened in reactor 2 and a considerable amount of diphenol was detected, while nothing happened in reactor 3. This again proved that phenoxy radicals were formed on the catalyst in reactor 1, and the 5 ml solution taken out from reactor 1 provided the phenoxy radicals which initiated the reaction chain in reactor 2 without an involvement of the catalyst. On the other hand, the absence of free radicals in the solution taken out from reactor 4 made the propagation of a reaction chain impossible in reactor 3.

Based on the intermediates formed in scheme 2, the following side reaction is perhaps the main side reaction, so the solution is darkened after reaction:

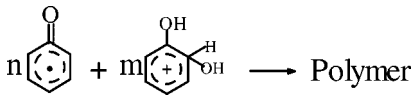

Scheme 3.

According to the mechanism in scheme 2, phenoxy radical formation on the catalyst surface is the initiation step of the reaction over the catalysts, and phenoxy radicals are involved in the propagation of the reaction chain. Therefore, the small crystallite size and high surface area of Fe–Mg–Si–O and Fe–Si–O are probably the causes for their short induction period and high phenol conversion in comparison to Fe–Mg–O and α-Fe_2O_3. On the other hand, the greater diphenol selectivity for Fe–Mg–O and Fe–Mg–Si–O catalysts is related to their crystal structure. In the spinel structure, there are cation vacancy sites which are absent in the corundum structure [30]. These cation vacancies are electron rich and make the surrounding oxygen ions more basic. The more basic oxygen ions can abstract a proton from the adsorbed diphenol radical ion to balance excess charge, enhancing the formation of the diphenol product and lowering the concentration of the diphenol radical ion in liquid phase. Thus, the side reaction (10) is reduced and the diphenol selectivity is increased.

5. Conclusions

Adding silica gel into the metal salt solution before co-precipitation with ammonia is an effective way to prepare metal oxide or complex oxide catalysts with small crystallite size and high surface area. In the Fe–Si–O and Fe–Mg–Si–O catalysts prepared by this method, nano-sized crystallites of α-Fe_2O_3 and $MgFe_2O_4$ are dispersed in a

silica matrix, which prevents the growth or sintering of the crystallites upon calcination. Fe–Mg–Si–O is an efficient catalyst for phenol hydroxylation in aqueous H_2O_2 solution, which exhibits high activity, high selectivity, short induction period and short reaction time.

The heterogeneously catalyzed aqueous-phase oxidation of phenol proceeds by a free-radical mechanism which involves initiation on the catalyst surface and homogeneous or heterogeneous propagation in the liquid. During the induction period phenoxy radicals are formed on the Fe-based oxide catalysts, and the phenoxy radicals initiate the reaction chain in the solution. The induction period is shortened with an increase in the surface area of the catalysts. The diphenol selectivity is enhanced on catalysts containing $MgFe_2O_4$ with spinel structure. The cation vacancies in the spinel structure of the catalysts promote the production of diphenols and inhibit the formation of tar-like polymer by-product.

Acknowledgement

We gratefully acknowledge the financial support from Shanghai Research Institute of Petrochemical Technology. The authors are grateful to Professor Y. Tang and Professor Dr. W.M. Hua of Fudan university for helpful discussions.

References

[1] H. Jeifert, W. Waldmann and W. Schweidel, Ger. Patent 2410742 (1975).
[2] P. Maggioni, US Patent 3914323 (1975).
[3] M. Taramasso, G. Perego and B. Notari, US Patent 4410501 (1983).
[4] A. Thangaraj, R. Kumar and P. Ratnasamy, Appl. Catal. 57 (1990) L1.
[5] J.S. Reddy, R. Kumar and P. Ratnassamy, Appl. Catal. 58 (1990) L1.
[6] J.S. Reddy and S. Sivasanker, Catal. Lett. 11 (1994) 241.
[7] M.A. Camblor, A. Corma, A. Martinez and J. Perez-Pariente, J. Chem. Soc. Chem. Commun. (1992) 589.
[8] K.R. Jiri, Z. Amost and H. Jiri, Collect Czech. J. Chem. Soc. Chem. Commun. 60 (1995) 451.
[9] P.R. Hari and A.V. Ramaswamy, Appl. Catal. A 93 (1993) 123.
[10] J.F. Yu, C.L. Zhang, Y. Yang and T.H. Wu, Chin. J. Catal. 18 (1997) 130.
[11] J.F. Yu, Y. Yang and T.H. Wu, Chem. J. Chin. Univ. 17 (1996) 126.
[12] Y. Yang, J.F. Yu, T.H. Wu and J.Z. Sun, Chin. J. Catal. 18 (1997) 230.
[13] S.M. Imamura, Gjjutsu 22 (1981) 201.
[14] M. Ai, J. Catal. 54 (1978) 223.
[15] A. Njnibeako, Prepr. Canad. Symp. Catal. 5 (1977) 170.
[16] N. Al-Hayck, Water Res. 19 (1985) 657.
[17] T.A. Tatarinova, Kinet. Katal. 23 (1985) 54.
[18] S. Goldstein, G. Czapski and J. Robani, J. Phys. Chem. 98 (1994) 6586.
[19] C.B. Lui, Z. Zhang, X.G. Yang and Y. Wu, J. Chem. Soc. Chem. Commun. (1996) 1019.
[20] R.B. Yang, F.S. Xiao, D. Wu, Y. Lui, S.L. Qiu and R.R. Xu, Catal. Lett. 49 (1997) 49.
[21] R.B. Yang, F.S. Xiao, D. Wu, Y. Wu, S.L. Qiu and R.R. Xu, Catal. Today 51 (1997) 39.
[22] D.Y. Wang, Z.Q. Liu and F.Q. Liu, Appl. Catal. A 174 (1998) 25.
[23] A.M. Gibson and W.J. Hightower, J. Catal. 41 (1976) 431.
[24] P. Scherrer, Gött. Nachr. 2 (1918) 98.
[25] G.B. David, L.S. Stuat, D.M. George, A.F. Gustavo and I. Enrique, J. Catal. 181 (1998) 57.
[26] A. Sadana and J.R. Katzer, J. Catal. 35 (1974) 140.
[27] C. Meyer, G. Clement and J.C. Balaceanu, in: *Proc. 3rd Int. Congr. on Catalysis*, Vol. 1 (1965) p. 184.
[28] C. Walling and R.A. Johnson, J. Am. Chem. Soc. 97 (1975) 363.
[29] T. Tagawa, Y.J. Seo and S. Goto, J. Mol. Catal. 78 (1993) 201.
[30] H.H. Kung, M.C. Kung and B.L. Xang, J. Catal. 69 (1981) 506.